

Analysis and Effects of Cytosolic Free Calcium Increases in Response to Elicitors in *Nicotiana plumbaginifolia* Cells

David Lecourieux,^{a,1} Christian Mazars,^b Nicolas Pauly,^b Raoul Ranjeva,^b and Alain Pugin^{a,2}

^aUnité Mixte de Recherche Institut National de la Recherche Agronomique–Université de Bourgogne, Biochimie, Biologie Cellulaire et Ecologie des Interactions Plantes-Microorganismes, 17 rue de Sully, BP 86510, 21065 Dijon cedex, France

^bUnité Mixte de Recherche Centre National de la Recherche Scientifique–Université Paul Sabatier, Signaux et Messages Cellulaires chez les Végétaux, Pole de Biotechnologies Végétales, 24 chemin de Borde Rouge, BP 17, Auzeville, 31326 Castanet-Tolosan, France

Cell suspensions obtained from *Nicotiana plumbaginifolia* plants stably expressing the apoaequorin gene were used to analyze changes in cytosolic free calcium concentrations ($[Ca^{2+}]_{cyt}$) in response to elicitors of plant defenses, particularly cryptogein and oligogalacturonides. The calcium signatures differ in lag time, peak time, intensity, and duration. The intensities of both signatures depend on elicitor concentration and extracellular calcium concentration. Cryptogein signature is characterized by a long-sustained $[Ca^{2+}]_{cyt}$ increase that should be responsible for sustained mitogen-activated protein kinase activation, microtubule depolymerization, defense gene activation, and cell death. The $[Ca^{2+}]_{cyt}$ increase in elicitor-treated cells first results from a calcium influx, which in turns leads to calcium release from internal stores and additional Ca^{2+} influx. H_2O_2 resulting from the calcium-dependent activation of the NADPH oxidase also participates in $[Ca^{2+}]_{cyt}$ increase and may activate calcium channels from the plasma membrane. Competition assays with different elicitors demonstrate that $[Ca^{2+}]_{cyt}$ increase is mediated by cryptogein–receptor interaction.

INTRODUCTION

Calcium as a ubiquitous internal second messenger can regulate diverse cellular processes in plants, conveying signals received at the cell surface to the inside of the cell through spatiotemporal concentration changes that are decoded by an array of Ca^{2+} sensors (Trewavas and Malhó, 1998; Zielinski, 1998; Sanders et al., 1999; Reddy, 2001). Under resting conditions, the cytosolic free calcium concentration ($[Ca^{2+}]_{cyt}$) is low, between 100 and 200 nM (Bush, 1995), 10^4 times less than that in the fluid surrounding the cell and 10^4 to 10^5 less than that in the vacuolar compartment, which is an intracellular calcium store.

In plants, $[Ca^{2+}]_{cyt}$ increase has been reported in response to various stimuli, including mechanical and low-temperature signals (Knight et al., 1991, 1992, 1996; van Der Luit et al., 1999), hypoosmotic shock (Taylor et al., 1996; Takahashi et al., 1997; Cessna et al., 1998), light (Shacklock et al., 1992; Baum et al., 1999), oxidative stress (Price et al., 1994; Pei et al., 2000), ozone (Clayton et al., 1999), hormones (Gilroy and

Jones, 1992; McAinsh et al., 1992), Nod factors (Ehrhardt et al., 1996), and elicitors (Knight et al., 1991; Mithöfer et al., 1999; Blume et al., 2000). Thus, Ca^{2+} apparently mediates different cell-specific processes in plant growth, development, and defense responses. How this common Ca^{2+} signaling links different signals to so many diverse and specific responses has been an area of intense research for many years. There is now evidence that the temporal and spatial nature and the amplitude of $[Ca^{2+}]_{cyt}$ changes (the calcium signature) caused by a given signal contribute to the specificity of the response (Trewavas, 1999; Knight, 2000). Moreover, the same signal induces different calcium signatures depending on the organ, the tissue, or the cell type in a tissue (McAinsh and Hetherington, 1998; Kiegle et al., 2000; Reddy, 2001). The origin of $[Ca^{2+}]_{cyt}$ increase (extracellular medium, organelle types, and/or both) also may be important in the physiological response (Knight et al., 1996; van Der Luit et al., 1999).

Plants normally are subjected to a large variety of microorganisms, such as fungi, bacteria, and viruses, and they have developed molecular systems to perceive signal molecules from pathogenic or symbiotic microorganisms and to convert them into an adaptive response. Efficient mechanisms for resisting invading pathogens include the hypersensitive reaction and systemic acquired resistance (Dangl et al., 1996; Ryals et al., 1996). Elicitins secreted by *Phytophthora* species are 10-kD proteins with 74% sequence

¹ Current address: University of Vienna Biocenter, Institute of Microbiology and Genetics, Dr Bohrgasse, A-1030 Vienna, Austria.

² To whom correspondence should be addressed. E-mail pugin@dijon.inra.fr; fax 03-80-69-32-26.

Article, publication date, and citation information can be found at www.plantcell.org/cgi/doi/10.1105/tpc.005579.

conservation that induce such defense systems in tobacco plants (Ricci et al., 1989; Bonnet et al., 1996). The mode of action of cryptogein, secreted by the oomycete *Phytophthora cryptogea*, has been investigated using tobacco (*Nicotiana tabacum* var Xanthi) cell cultures. The sequence of events triggered by cryptogein include its high-affinity binding on plasma membrane (PM) glycoprotein(s) (Wendehenne et al., 1995; Bourque et al., 1998, 1999), followed by the phosphorylation of a variety of proteins (Viard et al., 1994; Lecourieux-Ouaked et al., 2000). Manipulating the phosphorylation state of proteins by either staurosporine, a protein kinase inhibitor, or calyculin A, a protein phosphatase inhibitor, suppressed or mimicked cryptogein effects, respectively, establishing that reversible phosphorylation is a key process in the transduction pathway (Lecourieux-Ouaked et al., 2000).

Protein phosphorylation is followed by a large and sustained calcium influx (Tavernier et al., 1995) and subsequent calcium-dependent cellular responses, including (1) anion and K⁺ efflux (Blein et al., 1991; Pugin et al., 1997); (2) PM depolarization (Pugin et al., 1997); (3) activation of mitogen-activated protein kinases (MAPKs) (Lebrun-Garcia et al., 1998); (4) activation of a NADPH oxidase responsible for the transient production of active oxygen species (AOS) (Bottin et al., 1994; Pugin et al., 1997), cytosol acidification, and large changes in sugar metabolism (Pugin et al., 1997); (5) microtubule depolymerization (Binet et al., 2001); (6) phytoalexin synthesis (Milat et al., 1991); and, much later, (7) cell death (Binet et al., 2001). All of these effects were prevented when calcium influx was compromised either by a calcium chelator (EGTA) or a calcium surrogate (La³⁺). Moreover, decreasing the external Ca²⁺ concentration by adding EGTA or La³⁺ during treatments with cryptogein suppressed the biological effects of the elicitor, indicating that a sustained Ca²⁺ influx was necessary throughout the treatment. These results highlight the involvement of extracellular Ca²⁺ in this signaling process.

Taking into account the importance of [Ca²⁺]_{cyt} in signal transduction, we investigated the [Ca²⁺]_{cyt} changes in *Nicotiana plumbaginifolia* cells treated with different elicitors

that induce (cryptogein) or do not induce (oligogalacturonides [OGs]) cell death and analyzed the origin of [Ca²⁺]_{cyt} increase in relation to other events, including AOS production. We also investigated the physiological significance of cytosolic free-calcium increases. To address these questions, we used *N. plumbaginifolia* cells expressing aequorin in cytosol, the luminescence of which depends on free Ca²⁺ concentration. Our data indicate that cryptogein is typified by a biphasic [Ca²⁺]_{cyt} signature compared with four other oligosaccharide elicitors: OGs, laminarin, chitopentaose, and lipopolysaccharides. We further demonstrate that [Ca²⁺]_{cyt} increase depends on cryptogein interaction with its PM receptor and involves both calcium influx from the external medium and calcium mobilization from internal stores. Cryptogein-induced H₂O₂ production participates in this [Ca²⁺]_{cyt} increase through plasma membrane channel activation. Our data also indicate that the sustained calcium increase in cryptogein-treated cells is responsible for sustained MAPK activation, defense gene activation, and cell death.

RESULTS

Aequorin-transformed *N. plumbaginifolia* cell suspensions were generated from leaves of transformed *N. plumbaginifolia* plants obtained by Knight et al. (1991). Before studying the variations of [Ca²⁺]_{cyt} in response to elicitors, we determined the sensitivity of these cell suspensions to cryptogein. Our previous data had been obtained using cell suspensions from *N. tabacum* var Xanthi. Data shown in Table 1 indicate that although *N. plumbaginifolia* cells were less sensitive to cryptogein than *N. tabacum* cells, all of the responses induced by the elicitor were reproduced with similar response intensities and kinetics using 1 μM cryptogein instead 0.1 μM for *N. tabacum*. These data led us to consider the possibility that transformed *N. plumbaginifolia* cells were an appropriate material in which to investigate the cryptogein-induced variations of cytosolic free Ca²⁺.

Table 1. Comparison of Cryptogein Effects in *N. tabacum* and Aequorin-Transformed *N. plumbaginifolia* Cell Suspensions

Responses after 30 min of Treatment	<i>N. tabacum</i> Cells Treated with 0.1 μM Cryptogein	<i>N. plumbaginifolia</i> Cells Expressing Apoaequorin Treated with 1 μM Cryptogein
Ca ²⁺ influx (nmol/g fresh wt.)	140 ± 20	80 ± 30
Extracellular alkalinization (pH change)	1.45 ± 0.11	1.15 ± 0.08
AOS production (nmol H ₂ O ₂ /g fresh wt.)	1175 ± 126	1360 ± 144
MAPK activation	Yes (50 and 46 kD)	Yes (50 and 46 kD)
Microtubule disruption	Yes	Yes

Calcium influx was measured using ⁴⁵Ca²⁺ as a tracer (Tavernier et al., 1995). Extracellular pH changes were measured in cell suspensions (Tavernier et al., 1995). AOS production was monitored using chemiluminescence of luminol (Bourque et al., 1998). In-gel kinase assays were performed to analyze MAPK activation (Lebrun-Garcia et al., 1998). Microtubules were examined using classic fluorescence techniques and confocal microscopy (Binet et al., 2001). All experiments were performed at least three times.

Specific Changes in $[Ca^{2+}]_{cyt}$ in Response to Different Elicitors

In control *N. plumbaginifolia* cells, the bioluminescence counts yielded resting $[Ca^{2+}]_{cyt}$ values of 95 ± 25 nM ($n = 10$). At saturating concentrations, cryptogein or OGs induced a typical biphasic $[Ca^{2+}]_{cyt}$ increase in *N. plumbaginifolia* cells, each characterized by specific intensity, kinetics, and duration (Figure 1A). In cryptogein-treated *N. plumbaginifolia* cells, a lag phase of 90 to 120 s preceded a 6-min transient and rapid $[Ca^{2+}]_{cyt}$ increase, which peaked at 2.4 ± 0.17 μ M ($n = 10$) after 5 min, and then decreased to 0.35 μ M. The first peak was followed immediately by a second $[Ca^{2+}]_{cyt}$ increase, which reached 0.75 ± 0.07 μ M ($n = 10$) at 20 min after the beginning of the treatment and then decreased slowly but did not return to the background level even after ~ 2.5 h of treatment. At the same time, Ca^{2+} influx, as monitored by $^{45}Ca^{2+}$ accumulation, increased linearly within cryptogein-treated cells, reaching 51 ± 0.4 nmol Ca^{2+} /0.1 g fresh weight ($n = 3$) after 2.5 h of treatment (Figure 1B).

After a lag phase of ~ 20 s, OG treatment (Figure 1A) induced a first transient increase in $[Ca^{2+}]_{cyt}$, which peaked at 1.34 ± 0.35 μ M ($n = 10$), within 60 to 90 s before decreasing. A second transient increase in $[Ca^{2+}]_{cyt}$ occurred at 4 min after the beginning of treatment, with a maximum value of 0.9 ± 0.18 μ M ($n = 10$). Then, $[Ca^{2+}]_{cyt}$ returned to the resting value within 15 to 20 min. In cryptogein- or OG-treated cells, the magnitude of the Ca^{2+} response was dependent on the elicitor concentration (Figures 1C and 1D). For the first peak, the saturating concentration for cryptogein-induced $[Ca^{2+}]_{cyt}$ increase was ~ 500 nM, with a half-maximal effect at ~ 100 nM. The magnitude and duration of the sustained second phase were similar for cryptogein concentrations between 100 and 500 nM, with 100 nM being the saturating concentration (Figure 1C). With OGs, the maximal $[Ca^{2+}]_{cyt}$ increase was obtained using ~ 100 μ g/mL cell suspension (Figure 1D), and the intensities of both phases decreased equally with decreasing OG concentrations. Moreover, in elicitor-treated cells, the intensity of each peak of $[Ca^{2+}]_{cyt}$ depended on the extracellular Ca^{2+} concentration. In cryptogein-treated cells, 0.5 mM extracellular Ca^{2+} triggered the maximal $[Ca^{2+}]_{cyt}$ increases (Figure 1E), and extracellular Ca^{2+} concentrations > 1 mM reduced both peaks (data not shown). In OG-treated cells, the Ca^{2+} concentration increase of the first peak was maximal with 10 mM extracellular calcium, whereas the second peak reached an optimal value with 0.5 mM extracellular calcium (Figure 1F).

We sought to determine if oligosaccharide derivatives known to be elicitors are typified by the calcium signatures they induce. Laminarin (100 μ g/mL cell suspension), a linear β -1,3-glucan from the brown alga *Laminaria digitata* (Klarzynski et al., 2000), induced a $[Ca^{2+}]_{cyt}$ increase comparable to the first peak of the cryptogein $[Ca^{2+}]_{cyt}$ responses, with a shorter lag time (60 s against 90 to 120 s with cryptogein) and a maximum $[Ca^{2+}]_{cyt}$ increase reaching $1.62 \pm$

0.11 μ M ($n = 10$). Using a 10-fold higher concentration, laminarin stimulated two distinct peaks in $[Ca^{2+}]_{cyt}$ at 2 and 4 min, respectively, with maxima reaching 2.51 ± 0.15 μ M ($n = 10$) (Figure 2A). Chitooligosaccharides (chitopentaose) and lipopolysaccharides, both reported to be elicitors of defense responses in various plant species (Boller, 1995; Müller et al., 1998), yielded biphasic $[Ca^{2+}]_{cyt}$ increases with kinetics and magnitudes comparable to those of OGs (Figure 2B).

Receptor-Mediated $[Ca^{2+}]_{cyt}$ Increases in Tobacco Cells Treated with Elicitins

We previously demonstrated that four different elicitors (cryptogein, cinnamomin, parasiticein, and capsicein) bind to the same plasma membrane protein with comparable affinity (Bourque et al., 1998, 1999). All four elicitors triggered the same early events, but with different efficiencies. Regarding calcium influx, the relative potency was in the order cryptogein $>$ parasiticein $>$ capsicein $>$ cinnamomin (Bourque et al., 1998). Here, we first monitored the $[Ca^{2+}]_{cyt}$ increase induced by each elicitor in *N. plumbaginifolia* cells (Figure 3A). Used at the same concentration (1 μ M), capsicein, parasiticein, and cinnamomin triggered transient $[Ca^{2+}]_{cyt}$ increases that peaked at 0.92 ± 0.09 μ M ($n = 10$), 0.87 ± 0.10 μ M ($n = 10$), and 0.63 ± 0.08 μ M ($n = 10$), respectively. Then, $[Ca^{2+}]_{cyt}$ decreased slowly without reaching the basal $[Ca^{2+}]_{cyt}$ level after 1 h of treatment ($[Ca^{2+}]_{cyt} = 0.35 \pm 0.04$ μ M with capsicein-treated cells, 0.35 ± 0.05 μ M with parasiticein-treated cells, and 0.28 ± 0.04 μ M with cinnamomin-treated cells). To determine whether the cryptogein-induced $[Ca^{2+}]_{cyt}$ increases in *N. plumbaginifolia* cells depended on a preliminary interaction with plasma membrane binding sites, and taking into account the fact that elicitors bind on the same high-affinity sites, we monitored $[Ca^{2+}]_{cyt}$ increases during competition assays in vivo using the most efficient (cryptogein) and the less efficient (cinnamomin) elicitors. As expected, increasing concentrations of cinnamomin (1 to 10 μ M) decreased both cryptogein-induced $[Ca^{2+}]_{cyt}$ increases, triggering a progressive shift from a cryptogein-induced $[Ca^{2+}]_{cyt}$ signature toward a cinnamomin-induced $[Ca^{2+}]_{cyt}$ signature (Figure 3B). The concentration of cinnamomin that induced 50% inhibition of the cryptogein Ca^{2+} response was ~ 3 μ M (Figure 3C).

Mobilization of Extracellular and Intracellular Pools of Ca^{2+} in Cryptogein and OG Responses

Previous data indicated that both cryptogein and OGs induced a fast Ca^{2+} influx, which then triggered a wide array of responses (Mathieu et al., 1991; Tavernier et al., 1995; Pugin et al., 1997; Binet et al., 1998; Lebrun-Garcia et al., 1998; Lecourieux-Ouaked et al., 2000; Binet et al., 2001).

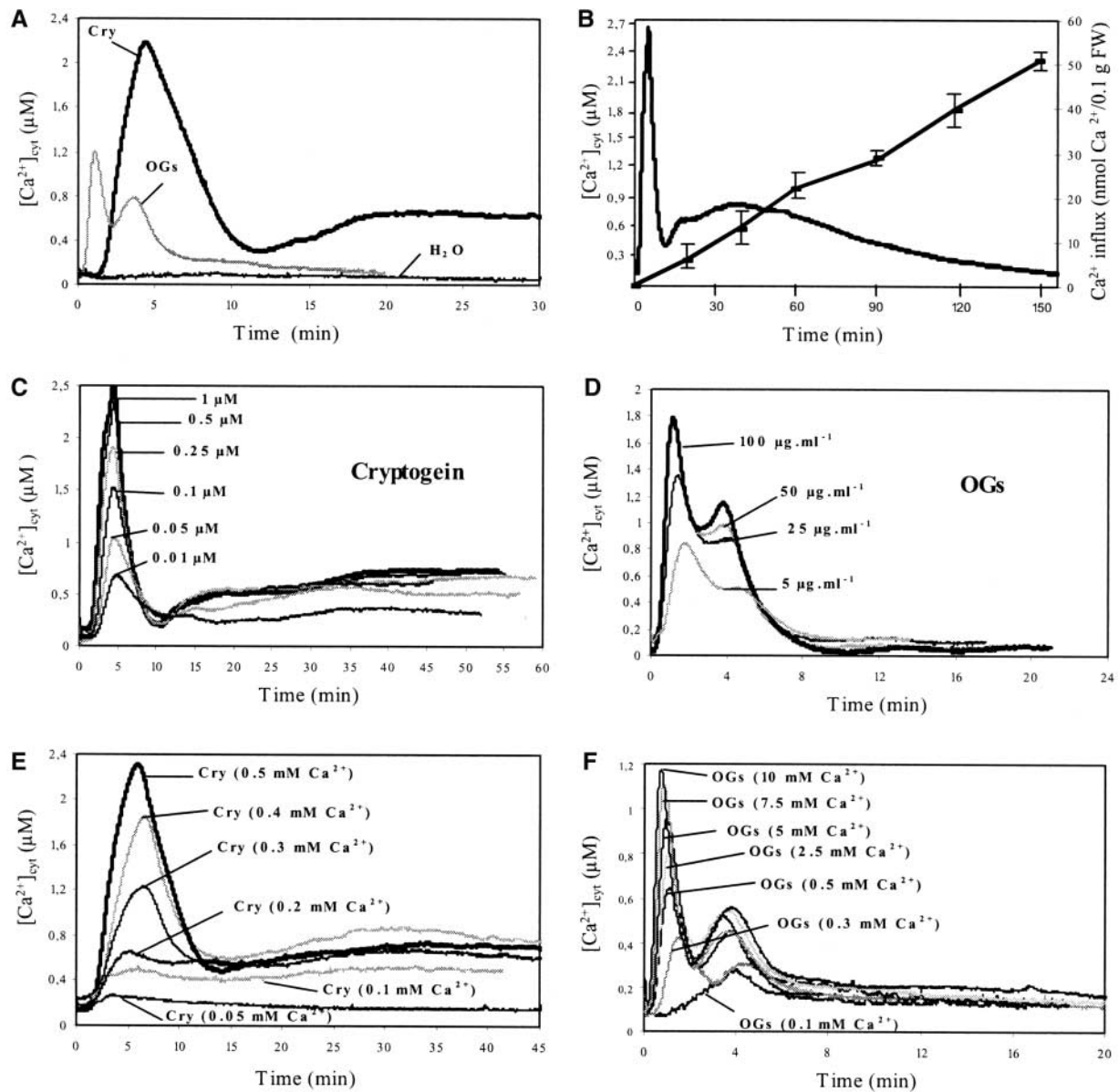


Figure 1. Changes in $[Ca^{2+}]_{cyt}$ in Aequorin-Transformed Cells during Treatment with Cryptogein or OGs.

(A) Treatment with H_2O , $1 \mu M$ cryptogein (Cry), or $100 \mu g/mL$ OGs.

(B) $^{45}Ca^{2+}$ influx and $[Ca^{2+}]_{cyt}$ changes in response to $1 \mu M$ cryptogein during a 3-h treatment.

(C) Dose-response relationships of $[Ca^{2+}]_{cyt}$ in cryptogein-treated cells.

(D) Dose-response relationships of $[Ca^{2+}]_{cyt}$ in OG-treated cells.

(E) Extracellular Ca^{2+} concentration dependence of cryptogein-induced $[Ca^{2+}]_{cyt}$ increase.

(F) Extracellular Ca^{2+} concentration dependence of OG-induced $[Ca^{2+}]_{cyt}$ increase.

Cryptogein treatment ($1 \mu M$) and OG treatment ($100 \mu g/mL$) were performed in medium containing different concentrations of Ca^{2+} , as indicated. Data correspond to 1 representative experiment of 10 experiments performed. Mean values \pm SE are given in the text. FW, fresh weight.

Here, we investigated the involvement of extracellular Ca^{2+} and of Ca^{2+} from internal stores in elicitor-induced $[\text{Ca}^{2+}]_{\text{cyt}}$ increases.

The addition of the calcium chelators 1,2-bis(*o*-aminophenoxy)ethane-*N,N,N,N*-tetraacetic acid (BAPTA; 2 mM) and EGTA (2 mM) in the extracellular medium suppressed $[\text{Ca}^{2+}]_{\text{cyt}}$ increases induced by both cryptogein (Figure 4A) and OGs (Figure 5B). Similarly, the calcium surrogates Gd^{3+} (1 mM) and La^{3+} (0.5 mM), added before cryptogein treatment, suppressed both peaks of cytosolic free Ca^{2+} (Figure 4B). Moreover, the addition of BAPTA or La^{3+} during cryptogein treatment rapidly decreased $[\text{Ca}^{2+}]_{\text{cyt}}$ to background levels independent of the time of addition (Figure 4C). These data indicate that this Ca^{2+} signature depends on a sustained Ca^{2+} influx from extracellular medium.

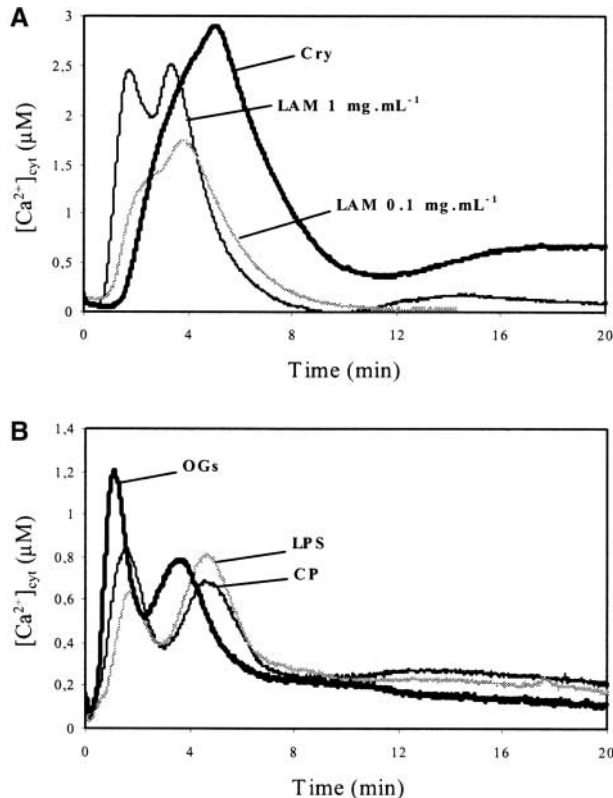


Figure 2. Effects of Different Elicitors on $[\text{Ca}^{2+}]_{\text{cyt}}$ Changes in Aequorin-Transformed Cells.

(A) Treatment with 1 μM cryptogein (Cry) and 0.1 or 1 mg/mL laminarin (LAM).

(B) Treatment with 100 $\mu\text{g}/\text{mL}$ OGs, 100 $\mu\text{g}/\text{mL}$ lipopolysaccharides (LPS), or 50 $\mu\text{g}/\text{mL}$ chitopentaoses (CP).

Data correspond to 1 representative experiment of 10 experiments performed. Mean values \pm SE are given in the text.

Subsequently, we determined the possible involvement of intracellular stores in the cryptogein- and OG-induced increases of $[\text{Ca}^{2+}]_{\text{cyt}}$ using neomycin, which inhibits phospholipase C and therefore the inositol 1,4,5-triphosphate (IP_3)-mediated Ca^{2+} release (Alexandre et al., 1990; Berridge, 1993; Allen et al., 1995; Franklin-Tong et al., 1996). At first, the efficiency of neomycin in inhibiting Ca^{2+} release from internal stores was verified by measuring their effects on mastoparan-treated cells. Indeed, mastoparan is known to activate phospholipase C, IP_3 production, and Ca^{2+} release from organelles in tobacco cells (Takahashi et al., 1998). Our results indicate that the mastoparan effect was prevented by neomycin (data not shown). In cryptogein-treated *N. plumbaginifolia* cells, neomycin (25 μM) reduced by $\sim 50\%$ the intensity of the first peak of $[\text{Ca}^{2+}]_{\text{cyt}}$ response and accelerated the peak of Ca^{2+} production between 5 and 3 min (Figure 5A). Assayed at 300 μM , neomycin was not more efficient at reducing the intensity of the first peak. In OG-treated cells, 25 μM neomycin clearly suppressed the second Ca^{2+} spike of the OG-induced $[\text{Ca}^{2+}]_{\text{cyt}}$ response; the first spike was unaffected (Figure 5B). This result suggests that in OG-treated cells, the first $[\text{Ca}^{2+}]_{\text{cyt}}$ increase, which peaked at ~ 1 min, results from extracellular Ca^{2+} influx, whereas the second peak at 4 min probably results from Ca^{2+} from internal stores. In the same manner, in cryptogein-treated cells, the first transient $[\text{Ca}^{2+}]_{\text{cyt}}$ increase, which peaked at 5 min, may correspond to two overlapping peaks of calcium from different origins: a first from external medium insensitive to neomycin, which peaked at ~ 3 min and corresponding to $\sim 50\%$ of the entire peak, and a second, inhibited by neomycin, that occurred later (between 3 and 8 min) and corresponding to Ca^{2+} from organelles. In cryptogein-treated cells, the second neomycin-insensitive sustained increase, which started after 15 min, could be attributable to the long-lasting influx of extracellular calcium.

Relationships between $[\text{Ca}^{2+}]_{\text{cyt}}$ Increase and Other Upstream and Downstream Responses in Elicitor-Treated Cells

Relationships with Protein Phosphorylation and MAPK Activation

Previous studies have reported the involvement of protein phosphorylation/dephosphorylation in the early steps of cryptogein signal transduction and characterized the phosphorylated proteins (Viard et al., 1994; Tavernier et al., 1995; Lecourieux-Ouaked et al., 2000). The protein kinase inhibitor staurosporine inhibited all of the effects induced by cryptogein, whereas these effects were induced by calyculin A (Lecourieux-Ouaked et al., 2000), an inhibitor of plant protein phosphatases 1 and 2A. The present data indicate that the cryptogein-induced $[\text{Ca}^{2+}]_{\text{cyt}}$ increase is inhibited completely by staurosporine (Figure 6).

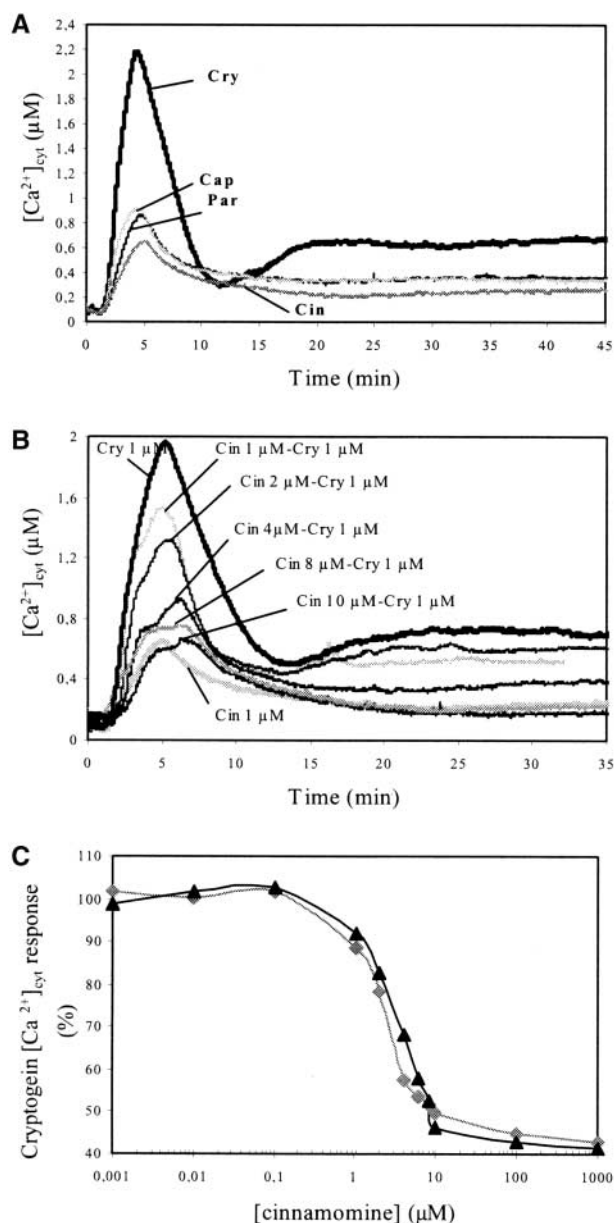


Figure 3. Effects of Four Elicitors on Changes in $[Ca^{2+}]_{cyt}$ in Aequorin-Transformed Cells and Competition Experiments using Cryptogein and Cinnamomin.

(A) Treatment with 1 μ M cryptogein (Cry), 1 μ M cinnamomin (Cin), 1 μ M parasiticein (Par), or 1 μ M capsaicin (Cap).

(B) In vivo competition experiments with 1 μ M cryptogein and increasing concentrations (0 to 10 μ M) of cinnamomin.

(C) Inhibition of cryptogein-induced $[Ca^{2+}]_{cyt}$ increase by increasing concentrations of cinnamomin during competition assays. The $[Ca^{2+}]_{cyt}$ response induced by 1 μ M cryptogein alone was referred to as 100%. The $[Ca^{2+}]_{cyt}$ response after 5 min (gray diamonds) or 30 min (black triangles) of cotreatment was calculated from **(B)**.

Data correspond to 1 representative experiment of 10 experiments performed. Mean values \pm SE are given in the text.

We previously reported a calcium influx-dependent activation of both MAPKs, salicylic-induced protein kinases (SIPKs), and wound-induced protein kinases (WIPKs), by cryptogein (Lebrun-Garcia et al., 1998). Here, we compared the kinetics of activation of SIPK and WIPK by cryptogein and OGs. Our data show a fast and sustained activation of MAPKs for at least 2 h in cryptogein-treated cells, whereas MAPK activation by OGs occurred early but did not exceed 15 min (Figure 7).

The same assays were performed in the presence of La^{3+} added 10 min after cryptogein treatment to check the involvement of the second sustained $[Ca^{2+}]_{cyt}$ increase in MAPK activation. In these conditions, the activation of SIPK and WIPK was suppressed (Figure 7).

Relationships with H_2O_2 Production

Although in cryptogein-treated cells, most events depend on Ca^{2+} influx, this does not exclude the possibility that in a second step, Ca^{2+} -dependent events amplify Ca^{2+} signaling by increasing Ca^{2+} influx and/or Ca^{2+} release from internal stores. In particular, H_2O_2 production from the Ca^{2+} -dependent activation of a NADPH oxidase (Tavernier et al., 1995; Pugin et al., 1997) could trigger a Ca^{2+} influx, as reported previously (Price et al., 1994; Levine et al., 1996; Takahashi et al., 1998; Kawano and Muto, 2000; Pei et al., 2000).

First, we investigated the effects of exogenous H_2O_2 on $[Ca^{2+}]_{cyt}$ using aequorin-expressing cells. The addition of H_2O_2 (10 mM) induced a typical biphasic $[Ca^{2+}]_{cyt}$ increase, with a first transient increase that peaked at ~ 1 min ($[Ca^{2+}]_{cyt} = 2.7 \pm 0.22 \mu$ M; $n = 10$) and lasted 5 min and a second sustained increase that started after 10 min, peaked at $\sim 1 \mu$ M (Figure 8A), and lasted for at least 2 h (data not shown). The intensity of the entire response depended on H_2O_2 concentration assayed between 1 and 10 mM. H_2O_2 -triggered $[Ca^{2+}]_{cyt}$ increase was abated totally in the presence of La^{3+} and decreased very slightly in the presence of the intracellular Ca^{2+} release antagonist neomycin (data not shown). Together, these results suggested that the $[Ca^{2+}]_{cyt}$ increase that followed H_2O_2 addition resulted mainly from extracellular Ca^{2+} influx.

In a second step, we investigated the contribution of cryptogein-induced H_2O_2 production to the increase of $[Ca^{2+}]_{cyt}$. Cells were cotreated with cryptogein and diphenylene iodonium, an inhibitor of the mammalian neutrophil NADPH oxidase (Cross and Jones, 1986), which is known to inhibit cryptogein-induced AOS production (Pugin et al., 1997). Alternatively, cells were cotreated with cryptogein and catalase (900 to 1800 units/mL cell suspensions), which immediately consumed H_2O_2 . The treatments with diphenylene iodonium (Figure 8B) and catalase (Figure 8C) had similar effects. In the absence of H_2O_2 , the intensity of the first cryptogein-induced transient $[Ca^{2+}]_{cyt}$ increase was reduced to $\sim 36\% \pm 7\%$ ($n = 10$), and this increase peaked earlier (2.5 instead of 5 min), suggesting that the first cryptogein-induced $[Ca^{2+}]_{cyt}$ increase resulted from at least two

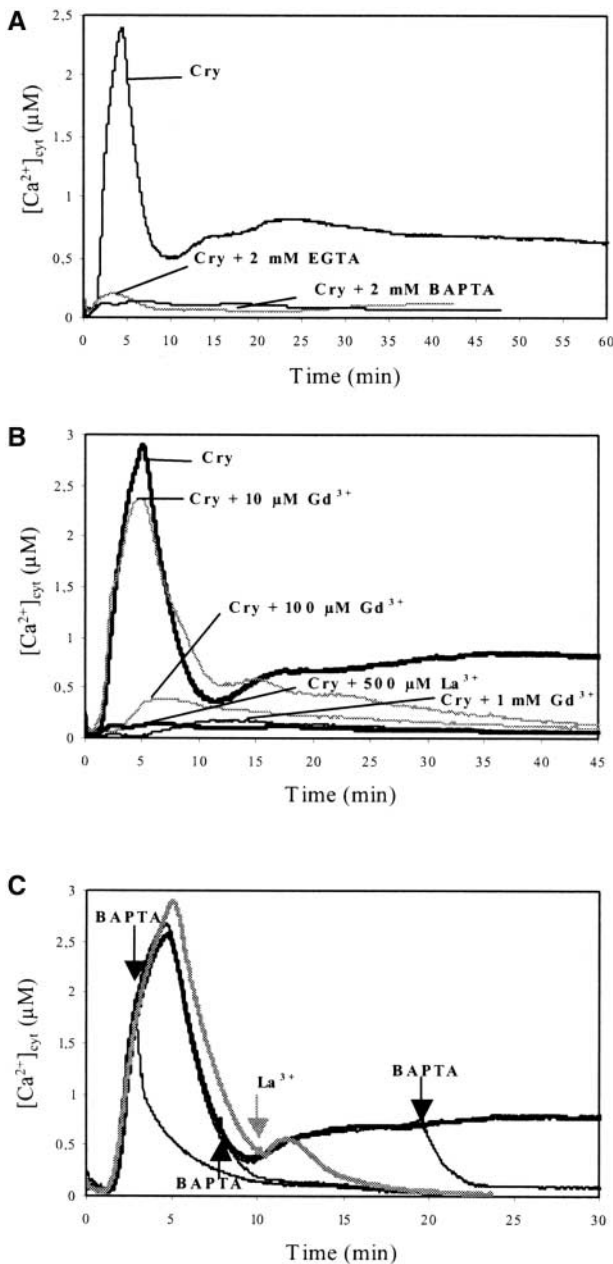


Figure 4. Involvement of Extracellular Ca^{2+} in Cryptogein-Induced $[Ca^{2+}]_{cyt}$ Increase in Aequorin-Transformed Cells.

(A) Effects of two Ca^{2+} chelators on changes in $[Ca^{2+}]_{cyt}$ in cells treated with 1 μM cryptogein. EGTA (2 mM) or BAPTA (2 mM) was added at 10 min before cryptogein (Cry) treatment.

(B) Effects of the Ca^{2+} channel surrogates $GdCl_3$ (Gd^{3+}) and $LaCl_3$ (La^{3+}) on changes in $[Ca^{2+}]_{cyt}$ in cells treated with cryptogein (1 μM). Gd^{3+} (10 μM to 1 mM) or La^{3+} (0.5 mM) was added at 10 min before cryptogein. The $[Ca^{2+}]_{cyt}$ curve obtained with 1 μM cryptogein was used as a reference.

(C) Inhibition of $[Ca^{2+}]_{cyt}$ increase by the addition of BAPTA or La^{3+} during cryptogein treatment (1 μM). BAPTA (2 mM) or La^{3+} (0.5 mM)

components; the second increase was caused by H_2O_2 . The long-sustained $[Ca^{2+}]_{cyt}$ increase in cryptogein-treated cells also was reduced in the presence of diphenylene iodonium or catalase (Figures 8B and 8C), indicating that H_2O_2 could participate in this sustained $[Ca^{2+}]_{cyt}$ increase. In OG-treated cells, in which the transient $[Ca^{2+}]_{cyt}$ increase clearly was dissociated into two peaks at 90 s and 4 min, respectively, diphenylene iodonium and catalase had similar effects, both compounds reducing the second peak (which was shown previously to be suppressed by neomycin), indicating that the corresponding $[Ca^{2+}]_{cyt}$ increase was mediated by H_2O_2 .

The $[Ca^{2+}]_{cyt}$ increase in the presence of catalase (9 to 15 min in cryptogein-treated cells, and 5 to 8 min in OG-treated cells; Figures 8C and 8D) probably results from the release of O_2 . Indeed, catalase alone had no effect (data not shown).

Relationship with Gene Expression and Cell Death

The *PAL* (Phe ammonia-lyase) gene encodes a key enzyme of the phenylpropanoid biosynthetic pathway (Dixon, 2001), and *hsr203J* expression has been related to the hypersensitive response (Marco et al., 1990; Pontier et al., 1994). Assuming that the second sustained $[Ca^{2+}]_{cyt}$ increase, triggered by cryptogein but not by oligosaccharide elicitors, was a determinant for defense response expression and particularly the hypersensitive reaction, we compared the kinetics of accumulation of both gene transcripts in cryptogein-treated cell suspensions with and without lanthanum or BAPTA added after 10 min of cryptogein treatment and in OG-treated cells. The data are presented in Figure 9. Cell death was estimated under the same conditions.

In cryptogein-treated cells, *PAL* and *hsr203J* mRNA levels increased as early as 1 h after treatment and persisted for at least 7 h. The addition of lanthanum at 10 min after treatment, before the second $[Ca^{2+}]_{cyt}$ increase, suppressed the accumulation of both gene transcripts. In OG-treated cells, *PAL* and *hsr203J* mRNA levels did not change compared with control levels. As reported previously both by others (Darvill and Albersheim, 1984; Mathieu et al., 1991) and ourselves (Binet et al., 2001), OGs did not induce any cell death. Proportions of cells that died after cryptogein treatment were $13\% \pm 2\%$, $21.5\% \pm 3\%$, $31\% \pm 4\%$, and $72\% \pm 2\%$ dead cells after 2.5, 5, 7.5, and 24 h, respectively.

was added as indicated by arrows. The cryptogein-induced $[Ca^{2+}]_{cyt}$ response was monitored as a control (thick black line).

Data correspond to 1 representative experiment of 10 experiments performed.

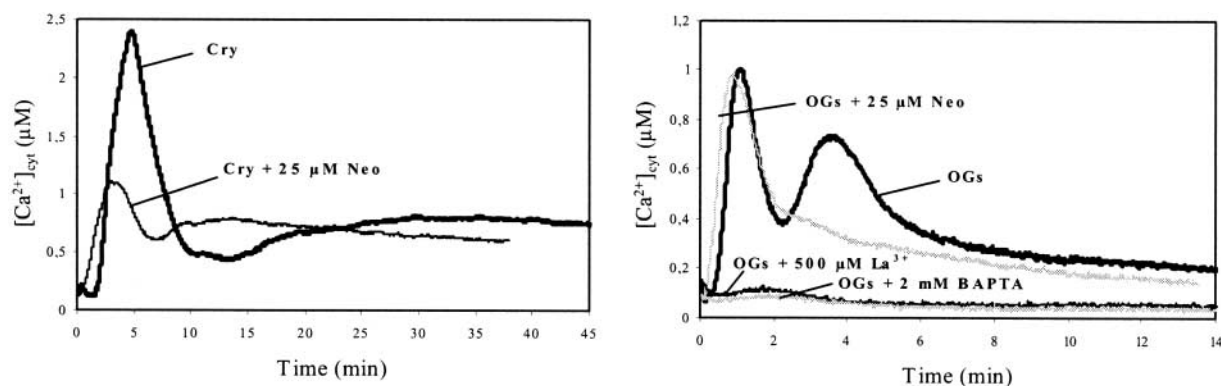


Figure 5. Effects of Neomycin on $[Ca^{2+}]_{cyt}$ Changes in Cryptogein- and OG-Treated Aequorin-Transformed Cells.

Cells were treated for 10 min with 25 μ M neomycin (Neo) before the addition of 1 μ M cryptogein (Cry) (A) or 100 μ g/mL OGs (B). Data correspond to 1 representative experiment of 10 experiments performed.

Control cell suspensions contained 2 to 4% dead cells during the 24-h assays. We reported previously that suppressing calcium influx by the addition of lanthanum before cryptogein treatment suppressed cell death (Binet et al., 2001). Here, our data indicate that the addition of 0.75 mM La^{3+} at 10 min after cryptogein addition also suppressed cell death. The proportion of dead cells after 5 h of culture was $3\% \pm 1\%$, $4\% \pm 2\%$, $21.5\% \pm 3\%$, and $5\% \pm 2\%$ in control cells, control cells with 0.75 mM La^{3+} , cryptogein-treated cells, and cryptogein-treated cell suspensions with lanthanum added at 10 min, respectively. Together, these results indicate that the sustained $[Ca^{2+}]_{cyt}$ increase in cryptogein-treated cells is involved in cell death.

DISCUSSION

$[Ca^{2+}]_{cyt}$ has been shown to play a key role in plant cell signal transduction. Particularly, the calcium signature of a given signal, characterized by its amplitude, duration, frequency, and location, was shown to encode a message that, after decoding by downstream effectors, contributes to the appropriate physiological response. The importance of $[Ca^{2+}]_{cyt}$ signals in the control of response pathways is well established in animals and plants (Dolmetsch et al., 1997; De Koninck and Schulman, 1998; McAinsh and Hetherington, 1998; Trewavas and Malhó, 1998; Allen et al., 2000). Cell suspensions, obtained from *N. plumbaginifolia* plants stably expressing the apoaequorin gene, were used to monitor and analyze $[Ca^{2+}]_{cyt}$ changes in response to elicitors and to investigate their origin and role. It was reported that the binding affinity and kinetic parameters of the aequorin protein could be altered by changes in intracellular monovalent ion concentration (Cessna et al., 2001). Thus, the $[Ca^{2+}]_{cyt}$ levels calculated by this method should be considered as estimates rather than exact values.

Cryptogein and Oligosaccharide Elicitors Trigger Specific $[Ca^{2+}]_{cyt}$ Signatures

Cryptogein and OGs trigger typical calcium signatures that differ in both kinetics (lag time, peak time, and duration) and peak intensities (Figure 1A). All three of the other oligosaccharide elicitors—laminarin, a β -1,3-glucan from the brown alga *Laminaria digitata* (Klarzynski et al., 2000), and chitooligosaccharides and lipopolysaccharides from *Pseudomonas* (Boller, 1995; Müller et al., 1998)—induced a signature resembling the OG response (Figure 2). The intensity of both cryptogein and OG signatures depends on elicitor concentration (Figures 1C and 1D) and on extracellular calcium concentration (Figures 1E and 1F). In cryptogein-treated cells, both $[Ca^{2+}]_{cyt}$ increases became larger with increasing extracellular calcium concentrations; 0.5 and 0.2 mM extracellular calcium saturated the response corresponding to the first transient peak and the second sustained phase, respectively (Figure 1E). Extracellular calcium concentrations >1 mM reduced the intensity of the first peak (data not shown).

This effect of high extracellular calcium concentrations is not the result of an inhibition of calcium influx, which increased linearly with increasing concentrations of extracellular calcium to 5 mM (data not shown). In OG-treated cells, the extent of the first $[Ca^{2+}]_{cyt}$ increase became larger with increasing extracellular calcium concentrations, 10 mM saturating this response, whereas the second $[Ca^{2+}]_{cyt}$ increase was optimal with 0.5 mM. Together, these data (Figures 1A, 1E, and 1F) suggest that cells activate new membrane components able to remove calcium from the cytosol when $[Ca^{2+}]_{cyt}$ approaches values greater than ~ 2.4 μ M. On the other hand, comparison of $[Ca^{2+}]_{cyt}$ and calcium influx (Figures 1A and 1B) indicates that a very low proportion of the calcium entering the cells is free. Indeed, considering that 1 g fresh weight of cells corresponds to ~ 1 mL (Pugin et al.,

1997), only 0.9% of the calcium that had penetrated the cells after 30 min of treatment was free in cytosol. This value decreased to 0.05% after 2.5 h. This observation highlights the ability of cells to buffer and store calcium in organelles and, particularly, the efficiency of vacuolar and endoplasmic reticulum Ca^{2+} -ATPases and $\text{Ca}^{2+}/\text{H}^{+}$ antiporters. The efficiency with which cells maintain low $[\text{Ca}^{2+}]_{\text{cyt}}$ for protracted periods demonstrates the functionality of the tonoplast and agrees with the long viability of cells ($\sim 10\%$ dead cells after 2.5 h of treatment) despite a large calcium influx and potentially damaging cellular events occurring from the first 5 min, including AOS production, anion efflux, PM depolarization, changes in sugar metabolism, and cytoskeleton depolymerization (see Introduction). These results also demonstrate that the prolonged and reversible phase of calcium response, which lasted 2 h (Figure 1B), is not a result of cell death.

Implication of Extracellular and Intracellular Pools of Ca^{2+} in Elicitor Responses and Involvement of H_2O_2

Using calcium chelators (EGTA and BAPTA) and calcium surrogates (La^{3+} and Gd^{3+}), we have shown that elicitor-induced $[\text{Ca}^{2+}]_{\text{cyt}}$ increases depend on a sustained calcium influx from external medium (Figure 4). This calcium influx then triggers calcium efflux from organelles, probably through IP_3 -activated calcium channels, as demonstrated indirectly by inhibiting the release of calcium from internal stores with neomycin (Figure 5). Calcium channels located on vacuolar and endoplasmic reticulum membranes (White, 2000), ligand gated by IP_3 (Schumaker and Sze, 1987; Alexandre et al., 1990), are involved in many physiological processes in plants (Sanders et al., 1999), especially in abscisic acid signaling (Wu et al., 1997; Leckie et al., 1998) and

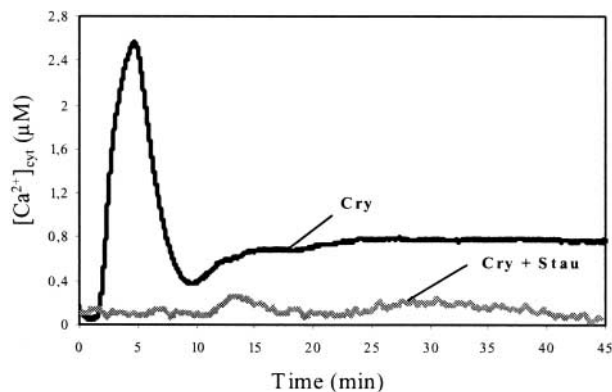


Figure 6. Effects of the Protein Kinase Inhibitor Staurosporine on Cryptogein-Induced $[\text{Ca}^{2+}]_{\text{cyt}}$ Changes in Aequorin-Transformed Cells.

Staurosporine (2 μM) was added 10 min before challenging cells with 1 μM cryptogein (Cry + Stau). Data correspond to 1 representative experiment of 10 experiments performed.

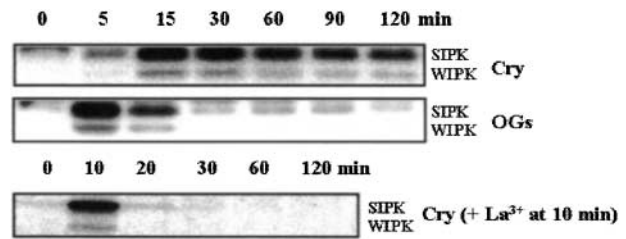


Figure 7. Time Course Activation of Both MAPKs, SIPK and WIPK, by 1 μM Cryptogein in the Presence or Absence of 0.5 mM La^{3+} Added 10 min after the Beginning of the Treatment or by OGs (100 $\mu\text{g}/\text{mL}$).

In-gel kinase assays were performed using myelin basic protein in the gel as a substrate and 30 μg of protein from cell extracts. MAPK activity was revealed using a buffer containing 40 mM Hepes, pH 7.5, 0.1 mM EGTA, 20 mM MgCl_2 , 2 mM DTT, 25 μM ATP, and 0.37 to 0.925 MBq of $\gamma\text{-}^{32}\text{P}$ -ATP (Amersham). Then, the gels were exposed to X-Omat AR film (Kodak). Data correspond to one representative experiment of three experiments performed. Cry, cryptogein.

plant defense (Durner et al., 1998; Mithöfer et al., 1999; Blume et al., 2000; Klessig et al., 2000).

We continued the analysis of the cryptogein calcium signature by determining the role of cryptogein-induced transient H_2O_2 production, which was detected after 3 min of treatment and peaked between 15 and 20 min (Lecourieux-Ouaked et al., 2000). H_2O_2 was shown to trigger calcium influx in tobacco (Price et al., 1994; Takahashi et al., 1998; Kawano and Muto, 2000), and $[\text{Ca}^{2+}]_{\text{cyt}}$ increase was reported to be involved in AOS-mediated cell death (Levine et al., 1996). Moreover, recent studies have reported that abscisic acid action was mediated by H_2O_2 -activated calcium channels in the PM of Arabidopsis guard cells (Pei et al., 2000). Our data indicate that exogenous H_2O_2 induced a biphasic $[\text{Ca}^{2+}]_{\text{cyt}}$ increase (Figure 8A) that could be attributable to an influx of extracellular Ca^{2+} . This $[\text{Ca}^{2+}]_{\text{cyt}}$ increase was suppressed by EGTA or La^{3+} but was not affected by neomycin (data not shown). Nevertheless, we do not exclude the contribution of neomycin-insensitive calcium release from internal stores as a result of H_2O_2 in addition to calcium influx. We also show that H_2O_2 produced in response to elicitors participates in the $[\text{Ca}^{2+}]_{\text{cyt}}$ increase. Indeed, NADPH oxidase inhibition (suppression of both O_2^- and H_2O_2) or H_2O_2 consumption in cryptogein- or OG-treated cells reduced or suppressed a peak of $[\text{Ca}^{2+}]_{\text{cyt}}$ increase. In both signatures, this peak corresponds kinetically to a peak that is reduced or suppressed in the presence of neomycin. Nevertheless, H_2O_2 produced by cells should not activate IP_3 -regulated channels from internal stores, as indicated by assays with exogenous H_2O_2 and neomycin.

Moreover, in cryptogein- or OG-treated cells, an additional Ca^{2+} influx could result from PM depolarization (Mathieu et al., 1991; Pugin et al., 1997). Voltage-dependent Ca^{2+} channels activated by membrane depolarization were

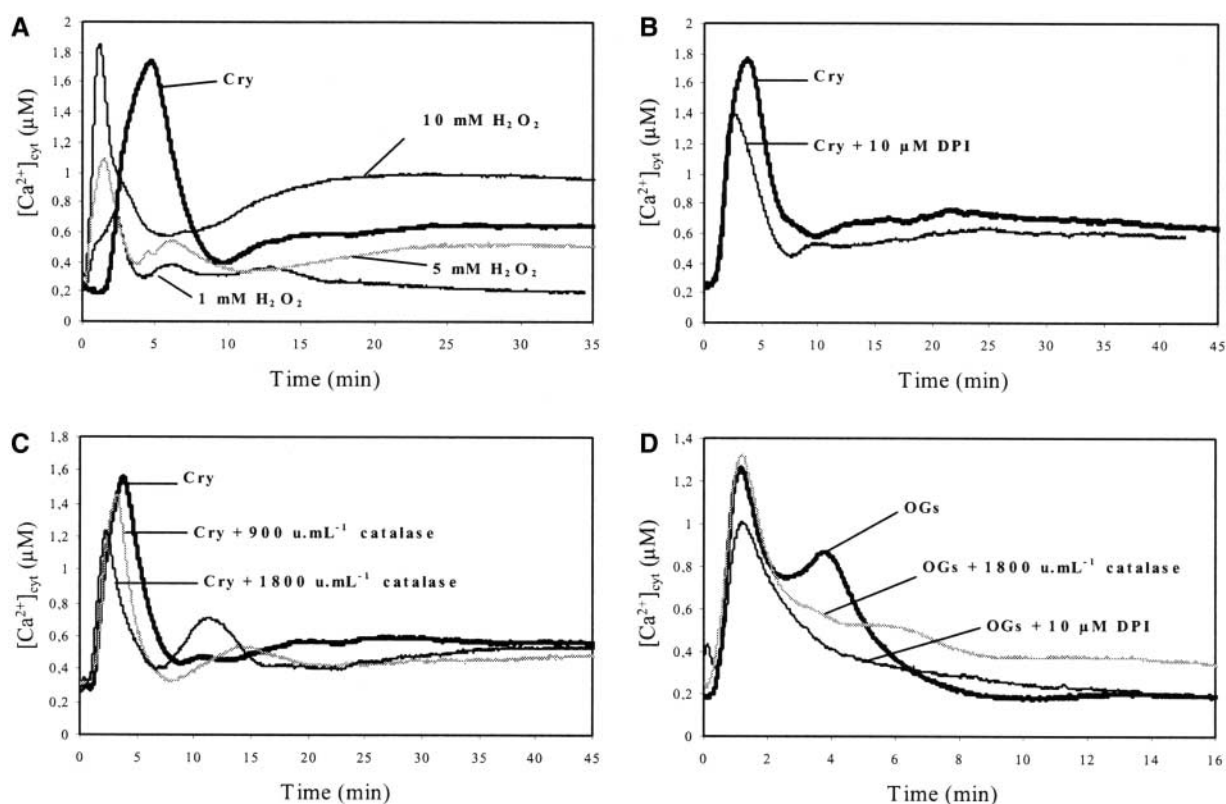


Figure 8. Involvement of H_2O_2 in Elicitor-Induced $[\text{Ca}^{2+}]_{\text{cyt}}$ Changes in Aequorin-Transformed Cells.

(A) Effects of exogenous H_2O_2 (1 to 10 mM) on $[\text{Ca}^{2+}]_{\text{cyt}}$ in cells compared with 1 μM cryptogein (Cry) treatment.

(B) Effects of diphenylene iodonium (DPI) on cryptogein-induced $[\text{Ca}^{2+}]_{\text{cyt}}$ changes in cells. Cells were incubated with 10 μM diphenylene iodonium for 10 min before the addition of 1 μM cryptogein.

(C) Effects of catalase on cryptogein-induced $[\text{Ca}^{2+}]_{\text{cyt}}$ changes in cells. Cells were treated for 15 min with catalase (900 and 1800 units/mL) before the addition of 1 μM cryptogein.

(D) Effects of diphenylene iodonium or catalase on OG-induced $[\text{Ca}^{2+}]_{\text{cyt}}$ changes in cells. Cells were treated for 10 min with 10 μM diphenylene iodonium or incubated for 15 min with catalase (1800 units/mL) before the addition of OGs (100 $\mu\text{g}/\text{mL}$).

Data correspond to 1 representative experiment of 10 experiments performed. Mean values \pm SE are given in the text.

identified on the PM (Pineros and Tester, 1997; White, 2000). Activation of voltage-dependent cation channels was reported in response to various signals, including blue and red light (Spalding and Cosgrove, 1989; Ermolayeva et al., 1996), Nod factors (Ehrhardt et al., 1992; Yokoyama et al., 2000), and fungal elicitors (Kuchitsu et al., 1993). In cryptogein-treated cells, the major calcium influx did not result from PM depolarization. Calcium influx occurred upstream and triggered anion efflux and PM depolarization (Pugin et al., 1997). Nitric oxide also may be involved in $[\text{Ca}^{2+}]_{\text{cyt}}$ increase. Cryptogein induced a very fast production of nitric oxide in tobacco cells (Foissner et al., 2000), and nitric oxide has been reported to trigger (1) calcium influx through cyclic GMP-dependent Ca^{2+} channels, (2) calcium release through cyclic ADPribose-dependent Ca^{2+} channels, and (3) direct activation of the ryanodine channel by *S*-nitrosylation in ani-

mal cells (reviewed by Wendehenne et al., 2001). Recent data highlight the involvement of cyclic nucleotide-gated ion channels (CNGC) in plant defense. Interestingly, the absence of functional AtCNGC2, a plasma membrane CNGC permeable to Ca^{2+} (Clough et al., 2000), characterizes the *Arabidopsis dnd1* mutant, which fails to produce the hypersensitive reaction in response to avirulent *Pseudomonas syringae* but expresses systemic acquired resistance constitutively (Yu et al., 1998).

$[\text{Ca}^{2+}]_{\text{cyt}}$ Increase Is Mediated by Cryptogein-Receptor Interaction

We sought to determine whether the cryptogein-induced $[\text{Ca}^{2+}]_{\text{cyt}}$ increase depends on receptor interaction, taking

advantages of four different elicitors that bind with comparable affinities to the same binding sites (Bourque et al., 1999). These triggered the same effects but with different magnitudes (Bourque et al., 1998). Competition assays in vivo using the most efficient elicitor (cryptogein) and increasing concentrations of the less efficient elicitor (cinnamomin) (Figure 3A) revealed a shift of the cryptogein calcium signature toward the cinnamomin calcium signature (Figure 3B). A cinnamomin concentration of 3 μM inhibited 50% of the cryptogein Ca^{2+} response (Figure 3C), consistent with the data reported by Bourque et al. (1998) and indicating that the concentration of elicitors inhibiting 50% of the effects of cryptogein in competition assays in vivo was approximately twice the concentration of cryptogein used. These results indicate that the typical $[\text{Ca}^{2+}]_{\text{cyt}}$ increase induced by cryptogein-treated cells depends on specific interactions with the high-affinity binding sites characterized previously (Bourque et al., 1999). In the same manner, $[\text{Ca}^{2+}]_{\text{cyt}}$ changes in parsley cells in response to the *Phytophthora sojae*-derived oligopeptide elicitor Pep-13 were shown to be receptor mediated (Blume et al., 2000). Inhibition of $[\text{Ca}^{2+}]_{\text{cyt}}$ increase by the protein kinase inhibitor staurosporine (Figure 6) indicates

that protein phosphorylation occurs upstream of the activation of PM calcium channels and could involve the receptor or associated proteins.

Effects of the Sustained $[\text{Ca}^{2+}]_{\text{cyt}}$ Increase in Cryptogein-Treated Cells

We reported previously a fast microtubule depolymerization in cryptogein-treated cells, whereas OGs had no effects. We also established that microtubule depolymerization was related to the intensity of calcium influx and to cell death (Binet et al., 2001). The relationship between the intensity of calcium influx, microtubule depolymerization, and cell death is reinforced by the present data, which show that laminarin, chitopentaose, and lipopolysaccharide, which did not trigger any sustained $[\text{Ca}^{2+}]_{\text{cyt}}$ (Figure 2), did not induce either microtubule depolymerization or cell death after 24 h of treatment (data not shown).

Our data demonstrate the involvement of the cryptogein-induced $[\text{Ca}^{2+}]_{\text{cyt}}$ increase in the sustained activation of MAPKs, in the accumulation of transcripts corresponding to

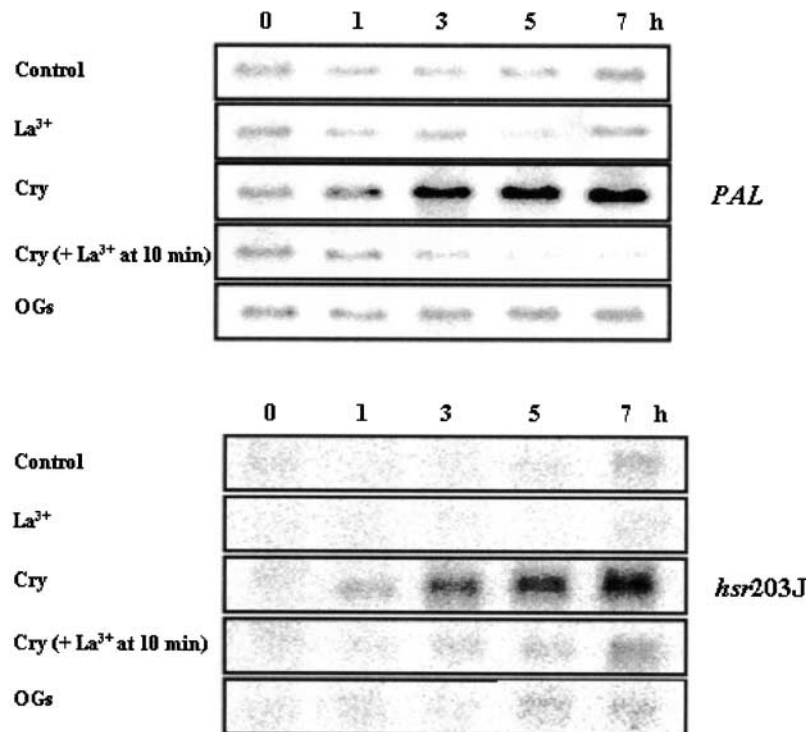


Figure 9. Time Course Accumulation of Transcripts of *PAL* and *hsr203J* Genes in OG- and Cryptogein-Treated Cells in the Presence or Absence of 0.5 mM La^{3+} Added 10 min after the Beginning of the Treatment.

Treatment doses were 100 $\mu\text{g}/\text{mL}$ OG and 1 μM cryptogein (Cry). RNA gel blot analysis was performed using 10 μg of total RNA per lane. Data correspond to one representative experiment of two experiments performed.

a defense gene (*PAL*) and to a gene associated with the hypersensitive cell death (*hsr203J*), and in cell death. Indeed, suppression of the sustained $[Ca^{2+}]_{cyt}$ increase in cryptogein-treated cells by the addition of lanthanum at 10 min after the beginning of the treatment suppressed the activation of both MAPKs (Figure 7), the accumulation of transcripts corresponding to *PAL* and *hsr203J* (Figure 9), and cell death. Interestingly, the SIPK/WIPK signaling cascade also has been reported to be involved in cryptogein-induced hypersensitive reaction activation (Zhang et al., 2000; Yang et al., 2001). The sustained activation of SIPK/WIPK caused by the maintained $[Ca^{2+}]_{cyt}$ increase might be explained by the continuous activation of the MAPK cascade and/or by the inhibition of negative regulators, including the protein phosphatase 2C-type phosphatase MP2C, which has been described as a negative regulator of SIPK/WIPK activation (Meskiene et al., 1998), and silenced by high $[Ca^{2+}]_{cyt}$ (Baudouin et al., 1999).

Thus, cryptogein receptor-mediated increase in $[Ca^{2+}]_{cyt}$ in *N. plumbaginifolia* cells depends on protein phosphorylation and involves successive influxes of extracellular calcium, probably through different types of PM calcium-permeable channels, and a release of calcium from intracellular stores. Activation of these calcium fluxes leads to a typical and well-defined calcium signature decoded by downstream effectors that, in conjunction with other second messengers, initiate a specific signaling cascade that leads to the appropriate physiological responses, hypersensitive reaction and systemic acquired resistance. The sustained increase that characterized the cryptogein signature, compared with oligosaccharide elicitors, may be involved in the hypersensitive reaction and cell death. Using different elicitors and tobacco cells, our research is now focused on the analysis of Ca^{2+} concentration changes in the nucleus and on the identification of downstream effectors such as protein kinases and transcriptional regulators.

METHODS

Aequorin-Transformed Tobacco Cells

Transformed *Nicotiana plumbaginifolia* plants (line MAQ2.4) expressing apoaequorin (Knight et al., 1991) were used to generate dark-grown cell suspensions as described previously (Chandra et al., 1997). Eight milliliters of aequorin-transformed cells was transferred to 100 mL of fresh liquid Chandler's medium (Chandler et al., 1972) every 8 days and maintained in dark-grown suspension by continuous shaking (150 rpm at 24°C). Transgenic tobacco (*Nicotiana tabacum*) cell suspensions behaved similarly to the untransformed *N. plumbaginifolia* cultures with respect to phenotype and growth kinetics. Before functional aequorin reconstitution and elicitor treatments, 8-day-old transgenic tobacco cell suspensions were collected and washed by filtration with a suspension buffer (175 mM mannitol, 0.5 mM $CaCl_2$, 0.5 mM K_2SO_4 , and 2 mM Hepes adjusted to pH 5.75). Cells were resuspended in suspension buffer to give a final concen-

tration of 0.1 g fresh weight/mL. In vivo reconstitution of aequorin was performed by the addition of 2 μ L of coelenterazine (5 mM stock solution in methanol) to 10 mL of cell suspension for at least 3 h in the dark (150 rpm at 24°C).

Cell viability was assayed using the vital dye neutral red as described by Binet et al. (2001). Cells (1 mL) were washed with 1 mL of a solution containing 175 mM mannitol, 0.5 mM $CaCl_2$, 0.5 mM K_2SO_4 , and 2 mM Hepes, pH 7.0, and then incubated for 5 min in the same solution supplemented with neutral red to a final concentration of 0.01%. Cells that did not accumulate neutral red were considered dying. At least 500 cells were counted for each treatment. The experiment was repeated three times.

Products

Elicitins were purified according to Bonnet et al. (1996) and were a gift from M. Ponchet (Institut National de la Recherche Agronomique, Antibes, France). Purified oligogalacturonides were a gift from M.A. Rouet-Mayer (Centre National de la Recherche Scientifique, Gif-sur-Yvette, France) and were used as a mixture of oligomers with degrees of polymerization ranging from 7 to 20. Laminarin, a linear β -1,3-glucan (degrees of polymerization from 25 to 30) from *Laminaria digitata*, was generously provided by Bernard Kloareg (Centre National de la Recherche Scientifique–Goëmar, Roscoff, France). Lipopolysaccharides (from *Pseudomonas aeruginosa*) were obtained from Sigma-Aldrich, and penta-*N*-acetylchitopentaose was obtained from Seikagaku America (Falmouth, MA). Coelenterazine was supplied by Calbiochem. Other chemicals were purchased from Sigma-Aldrich. When used, DMSO did not exceed a final concentration of 0.1%.

Aequorin Luminescence Measurements and Calibration

Bioluminescence measurements were made using a digital luminometer (Lumat LB9507; Berthold, Bad Wildbad, Germany). Cell culture aliquots (250 μ L) were transferred carefully to a luminometer glass tube, and the luminescence counts were recorded continuously at 1-s intervals (recorded as relative light units per second) and exported simultaneously (using Win Term software; Berthold) into Excel version 5.0 on a computer. Inhibitors, chelators, and control solvents were added at 15 min before elicitor treatments, with each volume of treatment not exceeding 1% of the cell aliquot volume.

In reconstituted aequorin control cells, the bioluminescence emission during a complete discharge of aequorin (with excess Ca^{2+}) was in the range of 1 to 2×10^5 relative light units \cdot s $^{-1}$ \cdot mg $^{-1}$ fresh weight. Approximately 40% of the reconstituted aequorin was consumed after 1 h of cryptogein treatment (1 μ M), against <5% after 1 h of oligogalacturonide treatment (50 μ g/mL cell suspension).

At the end of each experiment, residual functional aequorin was quantified by adding 300 μ L of lysis buffer (10 mM $CaCl_2$, 2% Nonidet P-40, and 10% ethanol) and monitoring the resulting increase in luminescence (until recordings returned to basal levels). Luminescence data transformation into cytosolic Ca^{2+} concentration was performed using the equation established by Allen et al. (1977), $[Ca^{2+}] = \{(L_0/L_{max})^{1/3} + [K_{TR}(L_0/L_{max})^{1/3}] - 1\} / \{K_R - [K_R(L_0/L_{max})^{1/3}]\}$, with K_R and K_{TR} values of 2×10^6 and 55 M^{-1} , respectively, as calculated by van Der Luit et al. (1999) using native coelenterazine and the specific aequorin isoform we used in these experiments at 22°C (our cell line was generated from MAQ2.4 transgenic plants, as used

by these authors). In this equation, L_0 is the luminescence intensity per second and L_{\max} is the total amount of luminescence present in the entire sample during the course of the experiment. Statistics on the magnitude of $[Ca^{2+}]_{\text{cyt}}$ peaks are given in the text as means \pm SE.

Except for diphenylene iodonium and catalase, all reagents used were tested previously on lysates containing recombinant aequorin to examine the direct effects of the reagent on aequorin luminescence (Haley et al., 1995; Sedbrook et al., 1996; Knight et al., 1996; Chandra et al., 1997; Sinclair and Trewavas, 1997; Blume et al., 2000). We tested diphenylene iodonium and catalase. None of these products interfered with aequorin luminescence.

RNA Gel Blot Analysis

Total RNA was isolated from tobacco cell suspensions using Trizol reagent (Gibco BRL) as described by the supplier. RNA gel blot analysis was performed using 10 μ g of total RNA per lane, separated on 1.2% agarose gels containing 1.1% formaldehyde. The gel was blotted to a nylon membrane (Hybond-XL; Amersham) and cross-linked by UV light. The probes for hybridization were labeled by random priming using the Ready-To-Go DNA Labeling Beads kit (without dCTP) from Amersham. The membrane was hybridized to the probes at 65°C and washed for 5 min with $2 \times$ SSC at room temperature ($1 \times$ SSC is 0.15 M NaCl and 0.015 M sodium citrate), once for 30 min at 65°C with 0.5% SDS and $2 \times$ SSC, and subsequently with $0.1 \times$ SSC for 30 min at room temperature. The membrane was exposed to a PhosphorImager screen, analyzed with a PhosphorImager Storm 880 (Molecular Dynamics, Sunnyvale, CA), and exposed to X-Omat AR film (Kodak).

In-Gel Kinase Assay

This technique was performed using the protocol described by Lebrun-Garcia et al. (1998) without modifications.

Upon request, all novel materials described in this article will be made available in a timely manner for noncommercial research purposes. No restrictions or conditions will be placed on the use of any materials described in this article that would limit their use for non-commercial research purposes.

ACKNOWLEDGMENTS

We are grateful to M.R. Knight and A.J. Trewavas for the *N. plumbaginifolia* line MAQ2.4. We thank M. Ponchet for the gift of cryptogein and Y. Marco for the *hstr203J* cDNA clone. We thank D. Wendehenne and A. Lebrun-Garcia for critical reading of the manuscript and A. Chiltz for in-gel kinase assays. We are grateful to K. Gould for reviewing the English manuscript. This work was supported by the Institut National de la Recherche Agronomique (INRA), Ministère de L'Enseignement Supérieur et de la Recherche, and the Conseil Régional de Bourgogne. D.L. was supported by a grant from the INRA and the Conseil Régional de Bourgogne.

Received June 21, 2002; accepted July 19, 2002.

REFERENCES

- Alexandre, J., Lassalles, J.P., and Kado, R.T. (1990). Opening of Ca^{2+} channels in isolated red beet root vacuole membrane by inositol 1,4,5-triphosphate. *Nature* **343**, 567–570.
- Allen, D.G., Blinks, J.R., and Prendergast, F.G. (1977). Aequorin luminescence: Relation of light emission to calcium concentration. A calcium-independent component. *Science* **195**, 996–998.
- Allen, G.J., Chu, S.P., Schumacher, K., Shimazaki, C.T., Vafeados, D., Kemper, A., Hawke, S.D., Tallman, G., Tsien, R.Y., Harper, J.F., Chory, J., and Schroeder, J.I. (2000). Alteration of stimulus-specific guard cell calcium oscillations and stomatal closing in *Arabidopsis det3* mutant. *Science* **289**, 2338–2342.
- Allen, G.J., Muir, S.R., and Sanders, D. (1995). Release of Ca^{2+} from individual plant vacuoles by both $InsP_3$ and cyclic-ADP-ribose. *Science* **268**, 735–737.
- Baudouin, E., Meskiene, I., and Hirt, H. (1999). Short communication: Unsaturated fatty acids inhibit MP2C, a protein phosphatase 2C involved in the wound-induced MAP kinase pathway regulation. *Plant J.* **20**, 343–348.
- Baum, G., Long, J.C., Jenkins, G.I., and Trewavas, A.J. (1999). Stimulation of the blue light phototropic receptor NPH1 causes a transient increase in cytosolic Ca^{2+} . *Proc. Natl. Acad. Sci. USA* **96**, 13554–13559.
- Berridge, M.J. (1993). Inositol triphosphate and calcium signalling. *Nature* **361**, 315–325.
- Binet, M.N., Bourque, S., Lebrun-Garcia, A., Chiltz, A., and Pugin, A. (1998). Comparison of the effects of cryptogein and oligogalacturonides on tobacco cells and evidence of different forms of desensitization induced by these elicitors. *Plant Sci.* **137**, 33–41.
- Binet, M.N., Humbert, C., Lecourieux, D., Vantard, M., and Pugin, A. (2001). Disruption of microtubular cytoskeleton induced by cryptogein, an elicitor of hypersensitive response in tobacco cells. *Plant Physiol.* **125**, 564–572.
- Blein, J.P., Milat, M.L., and Ricci, P. (1991). Responses of cultured tobacco cells to cryptogein, a proteinaceous elicitor from *Phytophthora cryptogea*: Possible plasmalemma involvement. *Plant Physiol.* **95**, 486–491.
- Blume, B., Nürnberger, T., Nass, N., and Scheel, D. (2000). Receptor-mediated increase in cytoplasmic free calcium required for activation of pathogen defense in parsley. *Plant Cell* **12**, 1425–1440.
- Boller, T. (1995). Chemoperception of microbial signals in plant cells. *Annu. Rev. Plant Physiol. Plant Mol. Biol.* **46**, 189–214.
- Bonnet, P., Bourdon, E., Ponchet, M., Blein, J.P., and Ricci, P. (1996). Acquired resistance triggered by elicitors in tobacco and others plants. *Eur. J. Plant Pathol.* **102**, 181–192.
- Bottin, A., Véronési, C., Pontier, D., Esquerré-Tugayé, M.T., Blein, J.P., Rustérucci, C., and Ricci, P. (1994). Differential responses of tobacco cells to elicitors from two *Phytophthora* species. *Plant Physiol. Biochem.* **32**, 373–378.
- Bourque, S., Binet, M.N., Ponchet, M., Pugin, A., and Lebrun-Garcia, A. (1999). Characterization of the cryptogein binding sites on plant plasma membranes. *J. Biol. Chem.* **274**, 34699–34705.
- Bourque, S., Ponchet, M., Binet, M.N., Ricci, P., Pugin, A., and Lebrun-Garcia, A. (1998). Comparison of binding properties and early biological effects of elicitors in tobacco cells. *Plant Physiol.* **118**, 1317–1326.
- Bush, D.S. (1995). Calcium regulation in plant cells and its role in signaling. *Annu. Rev. Plant Physiol. Plant Mol. Biol.* **46**, 95–122.

- Cessna, S.G., Chandra, S., and Low, P.S.** (1998). Hypo-osmotic shock of tobacco cells stimulates calcium fluxes deriving first from external and then internal calcium stores. *J. Biol. Chem.* **273**, 27286–27291.
- Cessna, S.G., Messerli, M.A., Robinson, K.R., and Low, P.S.** (2001). Measurement of stress-induced Ca^{2+} pulses in single aequorin-transformed tobacco cells. *Cell Calcium* **30**, 151–156.
- Chandler, M.T., Tandeau de Marsac, N., and Kouchkovsky, Y.** (1972). Photosynthetic growth of tobacco cells in liquid suspension. *Can. J. Bot.* **50**, 2265–2270.
- Chandra, S., Stennis, M., and Low, P.S.** (1997). Measurement of Ca^{2+} fluxes during elicitation of the oxidative burst in aequorin-transformed tobacco cells. *J. Biol. Chem.* **272**, 28274–28280.
- Clayton, H., Knight, M.R., Knight, H., McAinsh, M.R., and Hetherington, A.M.** (1999). Dissection of the ozone-induced calcium signature. *Plant J.* **17**, 575–579.
- Clough, S.J., Fengler, K.A., Yu, I.-C., Lippok, B., Smith, R.K., and Bent, A.F.** (2000). The *Arabidopsis dnd1* “defense, no death” gene encodes a mutated cyclic nucleotide-gated ion channel. *Proc. Natl. Acad. Sci. USA* **97**, 9323–9328.
- Cross, A.R., and Jones, O.T.G.** (1986). The effect of the inhibitor diphenylene iodonium on the superoxide-generating system of neutrophils: Specific labelling of a component polypeptide of the oxidase. *Biochem. J.* **237**, 111–116.
- Dangl, J.F., Robert, A.D., and Richberg, M.H.** (1996). Death don't have no mercy: Cell death programs in plant-microbe interaction. *Plant Cell* **8**, 1793–1807.
- Darvill, A., and Albersheim, P.** (1984). Phytoalexins and their elicitors: A defense against microbial infection in plants. *Annu. Rev. Plant Physiol.* **35**, 243–275.
- De Koninck, P., and Schulman, H.** (1998). Sensitivity of CaM kinase II to the frequency of Ca^{2+} oscillations. *Science* **279**, 227–230.
- Dixon, A.D.** (2001). Natural products and plant disease resistance. *Nature* **411**, 843–847.
- Dolmetsch, R.E., Lewis, R.S., Goodnow, C.C., and Healy, J.I.** (1997). Differential activation of transcription factors induced by Ca^{2+} response amplitude and duration. *Nature* **386**, 855–858.
- Durner, J., Wendehenne, D., and Klessig, D.F.** (1998). Defense gene induction in tobacco by nitric oxide, cyclic GMP, and cyclic ADP-ribose. *Proc. Natl. Acad. Sci. USA* **95**, 10328–10333.
- Ehrhardt, D.W., Atkinson, E.M., and Long, S.R.** (1992). Depolarization of alfalfa root hair membrane potential by *Rhizobium meliloti* Nod factors. *Science* **256**, 998–1000.
- Ehrhardt, D.W., Wais, R., and Long, S.R.** (1996). Calcium spiking in plant root hairs responding to *Rhizobium* nodulation signals. *Cell* **85**, 673–681.
- Ermolayeva, E., Holmeyer, H., Johannes, E., and Sanders, D.** (1996). Calcium-dependent membrane depolarisation activated by phytochrome in the moss *Physcomitrella patens*. *Planta* **199**, 352–358.
- Foissner, I., Wendehenne, D., Longterlaals, P., and Durner, J.** (2000). In vivo imaging of an elicitor-induced nitric oxide burst in tobacco. *Plant J.* **23**, 817–824.
- Franklin-Tong, V.E., Drobak, B.K., Allan, A.C., Watkins, P.A.C., and Trewavas, A.J.** (1996). Growth of pollen tubes of *Papaver rhoeas* is regulated by a slow-moving calcium wave propagated by inositol 1,4,5-triphosphate. *Plant Cell* **8**, 1305–1321.
- Gilroy, S., and Jones, R.L.** (1992). Gibberellic acid and abscisic acid co-ordinately regulate cytoplasmic calcium and secretory activity in barley aleurone protoplasts. *Proc. Natl. Acad. Sci. USA* **89**, 3591–3595.
- Haley, A., Russell, A.J., Wood, N., Allan, A.C., Knight, M., Campbell, A.K., and Trewavas, A.J.** (1995). Effects of mechanical signaling on plant cell cytosolic calcium. *Proc. Natl. Acad. Sci. USA* **92**, 4124–4128.
- Kawano, T., and Muto, S.** (2000). Mechanism of peroxidase actions for salicylic acid-induced generation of active oxygen species and an increase in cytosolic calcium in tobacco cell suspension culture. *J. Exp. Bot.* **51**, 685–693.
- Kiegle, E., Moore, C.A., Haseloff, J., Tester, M.A., and Knight, M.R.** (2000). Cell-type-specific calcium response to drought, salt and cold in the *Arabidopsis* root. *Plant J.* **23**, 267–278.
- Klarzynski, O., Plesse, B., Joubert, J.M., Yvin, J.C., Kopp, M., Kloareg, B., and Fritig, B.** (2000). Linear β -1,3 glucans are elicitors of defense responses in tobacco. *Plant Physiol.* **124**, 1027–1037.
- Klessig, D.F., et al.** (2000). Nitric oxide and salicylic acid signaling in plant defenses. *Proc. Natl. Acad. Sci. USA* **97**, 8849–8855.
- Knight, H.** (2000). Calcium signaling during abiotic stress in plants. *Int. Rev. Cytol.* **195**, 269–324.
- Knight, H., Trewavas, A.J., and Knight, M.R.** (1996). Cold calcium signaling in *Arabidopsis* involves two cellular pools and a change in calcium signature after acclimation. *Plant Cell* **8**, 489–503.
- Knight, M.R., Campbell, A.K., Smith, S.M., and Trewavas, A.J.** (1991). Transgenic plant aequorin reports the effects of touch and cold-shock and elicitors on cytoplasmic calcium. *Nature* **352**, 524–526.
- Knight, M.R., Smith, S.M., and Trewavas, A.J.** (1992). Wind-induced plant motion immediately increases cytosolic calcium. *Proc. Natl. Acad. Sci. USA* **89**, 4967–4971.
- Kuchitsu, K., Kikuyama, M., and Shibuya, N.** (1993). N-Acetylchito-oligosaccharides, biotic elicitors for phytoalexin production, induce transient membrane depolarization in suspension-cultured rice cells. *Protoplasma* **174**, 79–81.
- Lebrun-Garcia, A., Ouaked, F., Chiltz, A., and Pugin, A.** (1998). Activation of MAPK homologues by elicitors in tobacco cells. *Plant J.* **15**, 773–781.
- Leckie, C.P., McAinsh, M.R., Allen, G.J., Sanders, D., and Hetherington, A.M.** (1998). Abscisic acid-induced stomatal closure mediated by cyclic ADP-ribose. *Proc. Natl. Acad. Sci. USA* **95**, 15837–15842.
- Lecourieux-Ouaked, F., Pugin, A., and Lebrun-Garcia, A.** (2000). Phosphoproteins involved in the signal transduction of cryptogoin, an elicitor of defense reactions in tobacco. *Mol. Plant-Microbe Interact.* **13**, 821–829.
- Levine, A., Pennell, R.I., Alvarez, M.E., Palmer, R., and Lamb, C.** (1996). Calcium-mediated apoptosis in a plant hypersensitive disease resistance response. *Curr. Biol.* **6**, 427–437.
- Marco, Y., Raguesh, F., Godiard, L., and Froissard, D.** (1990). Transcriptional activation of 2 classes of genes during hypersensitive reaction of tobacco leaves infiltrated with an incompatible isolate of the phytopathogenic bacterium *Pseudomonas solanacearum*. *Plant Mol. Biol.* **15**, 145–154.
- Mathieu, Y., Kurkdijan, A., Xia, H., Guern, J., Koller, A., Spiro, M., O'Neill, M., Albersheim, P., and Darvill, A.** (1991). Membrane responses induced by oligogalacturonides in suspension-cultured tobacco cells. *Plant J.* **1**, 333–343.
- McAinsh, M.R., Brownlee, C., and Hetherington, A.M.** (1992). Visualizing changes in cytosolic Ca^{2+} during the response of stomatal guard cells to abscisic acid. *Plant Cell* **4**, 1113–1122.
- McAinsh, M.R., and Hetherington, A.M.** (1998). Encoding specificity in Ca^{2+} signalling systems. *Trends Plant Sci.* **3**, 32–36.
- Meskiene, I., Bogre, L., Glaser, W., Balog, J., Brandstotter, M.,**

- Zwerger, K., Ammerer, G., and Hirt, H. (1998). MP2C, a plant protein phosphatase 2C, functions as a negative regulator of activated protein kinase pathways in yeast and plants. *Proc. Natl. Acad. Sci. USA* **95**, 1938–1943.
- Milat, M.L., Ricci, P., and Blein, J.P. (1991). Capsidiol and ethylene production by tobacco cells in response to cryptogein. *Phytochemistry* **30**, 2171–2173.
- Mithöfer, A., Ebel, J., Bhagwat, A.A., Boller, T., and Neuhaus-Url, G. (1999). Transgenic aequorin monitors cytosolic transients in soybean cells challenged with β -glucan or chitin elicitors. *Planta* **207**, 566–574.
- Müller, P., Zähringer, U., and Rudolph, K. (1998). Induced resistance by bacterial lipopolysaccharides (LPS). In *Proceedings of the Ninth International Conference, Centre for Advanced Study in Botany, Plant Pathogenic Bacteria*. A. Mahadevan, ed (Madras, India: University of Madras), pp. 569–575.
- Pei, Z.M., Murata, Y., Benning, G., Thomine, S., Klüsener, B., Allen, A.J., Grill, E., and Schroeder, J.I. (2000). Calcium channels activated by hydrogen peroxide mediate abscisic acid signaling in guard cells. *Nature* **406**, 731–734.
- Pineros, M., and Tester, M. (1997). Characterization of the high-affinity verapamil binding site in a plant plasma membrane Ca^{2+} -selective channel. *J. Membr. Biol.* **157**, 139–145.
- Pontier, D., Godiard, L., Marco, Y., and Roby, D. (1994). *hsr203J*, a tobacco gene whose activation is rapid, highly localized and specific for incompatible plant/pathogen interactions. *Plant J.* **5**, 507–521.
- Price, A.H., Taylor, A., Ripley, S.J., Griffiths, A., Trewavas, A.J., and Knight, M.R. (1994). Oxidative signals in tobacco increase cytosolic calcium. *Plant Cell* **6**, 1301–1310.
- Pugin, A., Frachisse, J.M., Tavernier, E., Bligny, R., Gout, E., Douce, R., and Guern, J. (1997). Early events induced by the elicitor cryptogein in tobacco cells: Involvement of a plasma membrane NADPH oxidase and activation of glycolysis and the pentose phosphate pathway. *Plant Cell* **9**, 2077–2091.
- Reddy, A.S.N. (2001). Calcium: Silver bullet in signalling. *Plant Sci.* **160**, 381–404.
- Ricci, P., Bonnet, P., Huet, J.C., Sallantin, M., Beauvais-Canté, F., Bruneteau, M., Billard, V., Michel, G., and Pernollet, J.C. (1989). Structure and activity of proteins from pathogenic fungi *Phytophthora* eliciting necrosis and acquired resistance in tobacco. *Eur. J. Biochem.* **183**, 555–563.
- Ryals, J.A., Neuenschwander, U.H., Willits, M.G., Molina, A., Steiner, H.-Y., and Hunt, M.D. (1996). Systemic acquired resistance. *Plant Cell* **8**, 1809–1819.
- Sanders, D., Brownlee, C., and Harper, J.F. (1999). Communicating with calcium. *Plant Cell* **11**, 691–706.
- Schumaker, K.S., and Sze, H. (1987). Inositol 1,4,5-triphosphate releases Ca^{2+} from vacuolar membrane vesicles of oat roots. *J. Biol. Chem.* **262**, 3944–3946.
- Sedbrook, J.C., Kronebusch, P.J., Borisy, G.G., Trewavas, A.J., and Masson, P.H. (1996). Transgenic aequorin reveals organ-specific Ca^{2+} responses to anoxia in *Arabidopsis thaliana* seedlings. *Plant Physiol.* **111**, 243–257.
- Shacklock, P.S., Read, N.D., and Trewavas, A.J. (1992). Cytosolic free calcium mediates red-light induced photomorphogenesis. *Nature* **358**, 753–755.
- Sinclair, W., and Trewavas, A.J. (1997). Calcium in gravitropism: A re-examination. *Planta* **203** (suppl. 1), 85–90.
- Spalding, E.P., and Cosgrove, D.J. (1989). Large plasma membrane depolarisation precedes rapid blue-light-induced growth inhibition in cucumber. *Planta* **178**, 407–410.
- Takahashi, K., Isobe, M., and Muto, S. (1997). An increase in cytosolic calcium ion concentration precedes hypoosmotic shock-induced activation of protein kinases in tobacco suspension culture cells. *FEBS Lett.* **401**, 202–206.
- Takahashi, K., Isobe, M., and Muto, S. (1998). Mastoparan induces an increase in cytosolic calcium ion concentration and subsequent activation of protein kinases in tobacco suspension culture cells. *Biochim. Biophys. Acta* **1401**, 339–346.
- Tavernier, E., Wendehenne, D., Blein, J.P., and Pugin, A. (1995). Involvement of free calcium in action of cryptogein, a proteinaceous elicitor of hypersensitive reaction in tobacco cells. *Plant Physiol.* **109**, 1025–1031.
- Taylor, A.R., Manison, N.F.H., Fernandez, C., Wood, J., and Brownlee, C. (1996). Spatial organization of calcium signalling involved in cell volume control in the *Fucus* rhizoid. *Plant Cell* **8**, 2015–2031.
- Trewavas, A.J. (1999). Le calcium, c'est la vie: Calcium makes waves. *Plant Physiol.* **120**, 1–6.
- Trewavas, A.J., and Malhó, R. (1998). Ca^{2+} signalling in plant cells: The big network! *Curr. Opin. Plant Biol.* **1**, 428–433.
- van Der Luit, A.H., Olivari, C., Haley, A., Knight, M.R., and Trewavas, A.J. (1999). Distinct signaling pathways regulate calmodulin gene expression in tobacco. *Plant Physiol.* **121**, 705–714.
- Viard, M.P., Martin, F., Pugin, A., Ricci, P., and Blein, J.P. (1994). Protein phosphorylation is induced in tobacco cells by the elicitor cryptogein. *Plant Physiol.* **104**, 1245–1249.
- Wendehenne, D., Binet, M.N., Blein, J.P., Ricci, P., and Pugin, A. (1995). Evidence for specific high-affinity binding sites for a proteinaceous elicitor in tobacco plasma membrane. *FEBS Lett.* **374**, 203–207.
- Wendehenne, D., Pugin, A., Klessig, D.F., and Durner, J. (2001). Nitric oxide: Comparative synthesis and signaling in animal and plant cells. *Trends Plant Sci.* **6**, 177–183.
- White, P.J. (2000). Calcium channels in higher plants. *Biochim. Biophys. Acta* **1465**, 171–189.
- Wu, Y., Kuzma, J., Marechal, E., Graeff, R., Lee, H.C., Foster, R., and Chua, N.-H. (1997). Abscisic acid signaling through cyclic ADP-ribose in plants. *Science* **278**, 2126–2130.
- Yang, K.-Y., Liu, Y., and Zhang, Z. (2001). Activation of a mitogen-activated protein kinase pathway is involved in disease resistance in tobacco. *Proc. Natl. Acad. Sci. USA* **98**, 741–746.
- Yokoyama, T., Kobayashi, N., Kouchi, H., Minamisawa, K., Kaku, H., and Tsuchiya, K. (2000). A lipochito-oligosaccharide, Nod factor, induces transient calcium influx in soybean suspension-cultured cells. *Plant J.* **22**, 71–78.
- Yu, I.-C., Parker, J., and Bent, A. (1998). Gene-for-gene disease resistance without the hypersensitive response in *Arabidopsis dnd1* mutant. *Proc. Natl. Acad. Sci. USA* **95**, 7819–7824.
- Zhang, S., Liu, Y., and Klessig, D.F. (2000). Multiple levels of tobacco WIPK activation during the induction of cell death by fungal elicitors. *Plant J.* **23**, 339–347.
- Zielinski, R.E. (1998). Calmodulin and calmodulin-binding proteins in plants. *Annu. Rev. Plant Physiol. Plant Mol. Biol.* **49**, 697–725.